catalysts

MDPI

Article

Tailoring the Biochar Physicochemical Properties Using a Friendly Eco-Method and Its Application on the Oxidation of the Drug Losartan through Persulfate Activation

Alexandra A. Ioannidi [1], John Vakros [1,2], Zacharias Frontistis [3] and Dionissios Mantzavinos [1,*]

[1] Department of Chemical Engineering, University of Patras, Caratheodory 1, University Campus, GR-26504 Patras, Greece
[2] School of Sciences and Engineering, University of Nicosia, 2417 Nicosia, Cyprus
[3] Department of Chemical Engineering, University of Western Macedonia, GR-50132 Kozani, Greece
* Correspondence: mantzavinos@chemeng.upatras.gr

Abstract: In this study, spent malt rootlet-derived biochar was modified by a friendly eco-method using a low temperature (100 °C) and dilute acid, base, or water. The modification significantly enhanced the surface area from 100 to 308–428 m^2g^{-1} and changed the morphology and the carbon phase. In addition, the mineral's percentage and zero-point charge were significantly affected. Among the examined materials, the acid-treated biochar exhibited higher degradation of the drug losartan in the presence of persulfate. Interestingly, the biochar acted as an adsorbent at pH 3, whereas at pH = 5.6 and 10, the apparent kinetic constant's ratio $k_{oxidation}/k_{adsorption}$ was 3.73 ± 0.03, demonstrating losartan oxidation. Scavenging experiments indirectly demonstrated that the role of the non-radical mechanism (singlet oxygen) was crucial; however, sulfate and hydroxyl radicals also significantly participated in the oxidation of losartan. Experiments in secondary effluent resulted in decreased efficiency in comparison to pure water; this is ascribed to the competition between the actual water matrix constituents and the target compound for the active biochar sites and reactive species.

Keywords: biochar; activated persulfate; micropollutants; oxidation; adsorption; tailoring; losartan; physicochemical properties; correlation

Citation: Ioannidi, A.A.; Vakros, J.; Frontistis, Z.; Mantzavinos, D. Tailoring the Biochar Physicochemical Properties Using a Friendly Eco-Method and Its Application on the Oxidation of the Drug Losartan through Persulfate Activation. *Catalysts* **2022**, *12*, 1245. https://doi.org/10.3390/catal12101245

Academic Editor: Grzegorz Boczkaj

Received: 27 September 2022
Accepted: 12 October 2022
Published: 15 October 2022

1. Introduction

In recent years, a holistic approach has been increasingly followed to address environmental issues. New technologies are developed, while older ones are modified in the context of circular economy to deal with problems, such as the pollution of aquatic environments [1]. An idea that has attracted the scientific community's interest is the utilization of agricultural or industrial residues to produce valuable products. This approach is even more interesting if these products can be used to restore the environment, thus, significantly reducing the environmental footprint [2,3]. Biochar (BC) is a leading product of this kind; it can be derived from different raw materials such as agro-biochemical residues, biomass, and combustion sludge from wastewater treatment plants [4]. The first studies regarding the use of biochar dealt with its production from different biomass sources and subsequent application as a cheap and environmentally friendly adsorbent material [5]. Several studies have demonstrated biochar adsorption capacity removing different inorganic and organic pollutants such as toxic metals, azo dyes, pesticides, ammonia, and pharmaceuticals to replace the widely used activated carbon [5,6].

At the same time, there has been a tremendous increase in the research of carbocatalysis for environmental or energy applications [7]. Various researchers initially used catalysts made of ideal carbon materials such as carbon nanotubes, synthetic diamonds [8], carbon black [9], and graphene [10], with encouraging results. Based on these studies, many researchers have moved on to investigate the application of cheap and abundant biochar

for catalytic applications, with particular emphasis, in recent years, on using biochar from various sources to activate oxidants such as persulfate for the degradation of recalcitrant pollutants in the aqueous phase [11–15]. Indeed, using efficient catalytic materials that do not contain noble/expensive metals have been the holy grail for researchers dealing with the applications of catalysis in environmental protection. Although there are several studies on the performance of these systems in the aqueous phase, significant work is still needed in the field of optimization, but mainly in the synthesis/modification and tailoring of biomass-derived catalytic materials and correlation with their catalytic activity, ideally in conditions that represent environmental problems [16].

In previous studies of our group, it was found that biochar from spent malt rootlets was very efficient for the activation of persulfate ions and the oxidation of persistent organic contaminants such as sulfamethoxazole and trimethoprim [11,17]. This BC has a moderate specific surface area (SSA) of 100 m^2g^{-1} and equally balanced micropores and meso-macropores. Moreover, the prepared BC has a significant amount of minerals (i.e., 32%), which are mainly in the form of phosphoric, carbonates, and oxides of K, Ca, and Mg. The preparation conditions of biochar can influence greatly its physicochemical properties and, eventually, its ability as an adsorbent and/or activator, while the properties of the target compound may also dictate removal efficiency. For example, we have recently demonstrated [18] that the calcination temperature could alter the properties and, subsequently, the observed activity of BC from rice husk; the latter was strongly dependent on the type of antibiotic tested. This interesting point is not yet fully explored in the literature, where it is difficult to find comparative studies with BC prepared from the same raw biomass under the same pyrolysis temperature, but with different physicochemical properties. An interesting approach to modify the biochar is to mix an activator such as KOH, ZnO, K_2CO_3 [19–21] with biochar or biomass and then pyrolyze the mixed phase. This procedure usually produces biochar with high SSA. However, it is not so eco-friendly since it demands high temperatures, and dangerous side-products are produced. Thus, it will be interesting to find a more environmentally and energy friendly alternative procedure. Treatment with dilute acid or base solution, or even pure water, can be applied to modify the biochar under mild conditions, of approximately 100 °C, where the solutions boil.

In this study, we explore the oxidation of the antihypertensive drug losartan (LOS) through the biochar-driven activation of persulfate ions. Specifically, a BC from spent malt rootlets prepared by pyrolysis at 850 °C is modified with acid, base, or water under mild conditions to regulate its physicochemical properties, surface groups, and acidity. The proposed process modification leads to BC with extremely different properties. It is expected to exhibit different performances in the oxidation process, as it was proven for the transesterification reaction in biodiesel production [22]. The modification with acid, base, or pure water will cause changes in the surface acidity, carbon phase, and minerals speciation, while it will change the SSA of the samples. All these changes are expected to affect the BC performance significantly. They will further help researchers (i) to better understand the parameters responsible for the high activity of the BC and (ii) to tailor the properties of the BC to obtain catalytic materials with higher efficiency and/or for specific applications.

2. Results and Discussion

The effect of various BC treatments on its SSA is depicted in Table 1. Indeed, the moderate SSA of the starting BC increases considerably, e.g., more than 400% for the acid-treated BC, and even 300% for the water-treated one. The micropore's surface area also increases, from 58 m^2g^{-1} for the starting BC to 190 m^2g^{-1} in the acid-treated sample.

The SEM images of the various samples are presented in Figures S1–S4; as seen in Figure S1, the untreated, pristine BC keeps the rootlet shape, while macropores between 4 and 5 μm can be observed. In addition, there are many mineral deposits on the surface of BC. Treatment with H_2SO_4 alters the surface of BC. It makes the organic phase rough and dissolves part of it. This can clearly be seen in Figure S2, where holes can be detected in the

carbonaceous phase, while minerals are limited. In Figure S3, SEM images of base-treated BC samples are presented. There is also a rough surface due to the NaOH treatment. In this case, the minerals are more than the acid-treated BC, but less than the starting BC. Moreover, the macropores seem to be larger than the starting BC. The effect of water treatment on BC is less pronounced than the other two. A significant amount of minerals can still be detected, while the surface is less rough, presumably due to the mild treatment in the absence of an acid or base solution.

Table 1. Physicochemical properties of the starting and modified biochars.

Sample	SSA (m^2g^{-1})	Micropores SSA (m^2g^{-1})	pzc	Minerals (%)	TGA Temp. (°C)
BC	100	58	8.2	32	476
Acid–BC	428	190	<2.5	3	570
Base–BC	362	175	9.5	13	451
Water–BC	308	142	7.2	24	462

Combining the results from SSA measurements and SEM images, one can see that treatment with acid or base is highly effective to increase SSA values. Indeed, the differences observed can be attributed to the dissolution of the minerals, especially in the acid treatment, which can unblock part of the meso-macropores and the removal of different species of the carbonaceous phase. The last mechanism is responsible for the microporosity, although different parts of the carbonaceous phase are dissolved in the acid or base treatment.

Additionally, the TGA curves of the biochars under air atmosphere are informative, as presented in Figure 1. Oxygen burns the carbonaceous phase and releases CO_2, leaving the minerals in the mass balance. The mass left after TGA is reported in Table 1 and corresponds to the mineral content in each BC. It confirms the removal of inorganic species during treatment.

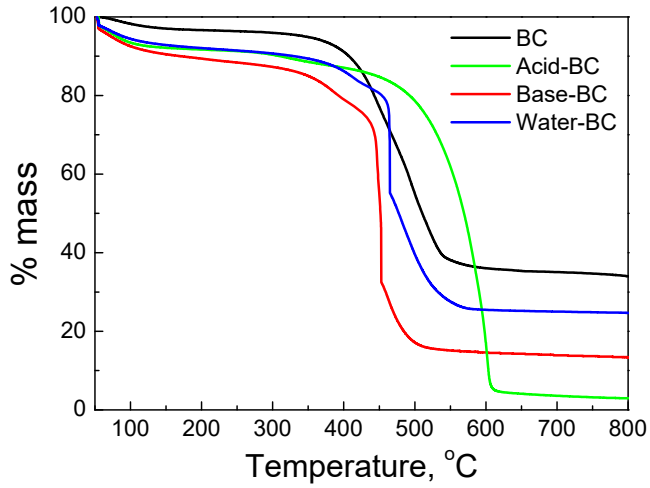

Figure 1. TGA curves of the studied biochars. The run was carried out under air atmosphere at 20 mL/min flowrate.

The TGA curve of each biochar has a slight mass loss at low temperatures in the range of 80–130 °C, corresponding to the water adsorbed, and a sharp decrease in higher temperatures, thus, describing the burn of the carbonaceous phase. The starting temperature is different in each biochar and depends on the physicochemical characteristics of the carbonaceous phase. A higher burning temperature is required for the more solid and massive phases produced from lignin, while hemicellulose and cellulose demand lower burning temperatures. In this case, the acid–BC exhibits the higher and the base–BC exhibits the lower burning temperature, while the starting biochar and water–BC are in between

(Table 1). As can be seen, there are significant differences, which can be attributed to the influence of the treatment. It is well known that acid solutions can dissolve hemicellulose and cellulose species in biomass, while base solutions are used to remove lignin. Although the pyrolysis process alters the characteristics of biomass and graphitizes the carbon phase, this phase's characteristics are related to the starting biomass. Treatment with acid or base solutions can alter the speciation and transform the carbonaceous phase to a harder- or easier-to-burn phase. The partially dissolved biochar is also supported by the SEM images (Figures S2 and S3).

Treatment also affects the surface groups of the biochars. These groups, mainly surface O species, are responsible for the acid–base behavior of the biochar in a solution and participate in almost all surface processes, such as adsorption, SPS activation, and oxidation of organic contaminants. The results of the potentiometric titrations are presented in Figure 2, and the pzc values are reported in Table 1. As can be seen, the pzc value of the starting biochar is 8.2 and increases after base treatment to 9.5, while it shifts to extremely low values for the acid-treated sample. The water–BC sample exhibits only a small shift in the pzc, probably due to the removal of some basic minerals dissolved by the boiling water.

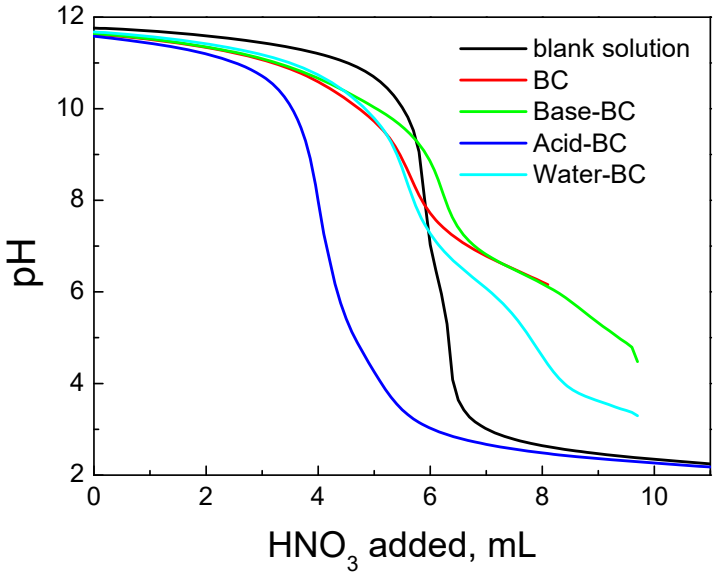

Figure 2. Potentiometric titrations of the studied biochars with the titration of the blank solution.

The significant differences in the physicochemical properties of the treated biochars are expected to alter the catalytic performance of the materials. Specifically, the influence of biochar and treated biochars with different physicochemical properties on LOS adsorption and oxidation with persulfate ions was investigated, and the results are displayed in Figure 3. As seen in Figure 3A, the 90 min removal by adsorption of 250 μg/L LOS is 9.8%, 16.5%, 9.8%, and 42% for BC, water–BC, base–BC, and acid–BC, respectively, at inherent pH. There are two different processes during the immersion of biochar into the LOS solution: (i) the consumption or release of H^+ ions from the surface depending on the difference of the pH solution and the pzc of the biochar, and more importantly, (ii) the adsorption of LOS. If the adsorption is due to electrostatic forces and not to π–π interactions, then charged groups are involved in the process, and depending on the accumulation of charge on the surface, H^+ may be released or consumed by the surface. Thus, the solution pH will be altered. In this case, the starting solution is lower for acid–BC and water–BC (pH = 4.6 and 5.2, respectively), but higher for BC and base–BC (pH = 6.0 and 6.2, respectively). This points out that the adsorption is followed by H^+ released from the surface and is favored at a lower pH. The pH increase for BC and base–BC is due to the basicity of the two samples, which firstly increases the pH and then limits the adsorption process, and thus, the acidification of the solution by the release of H^+.

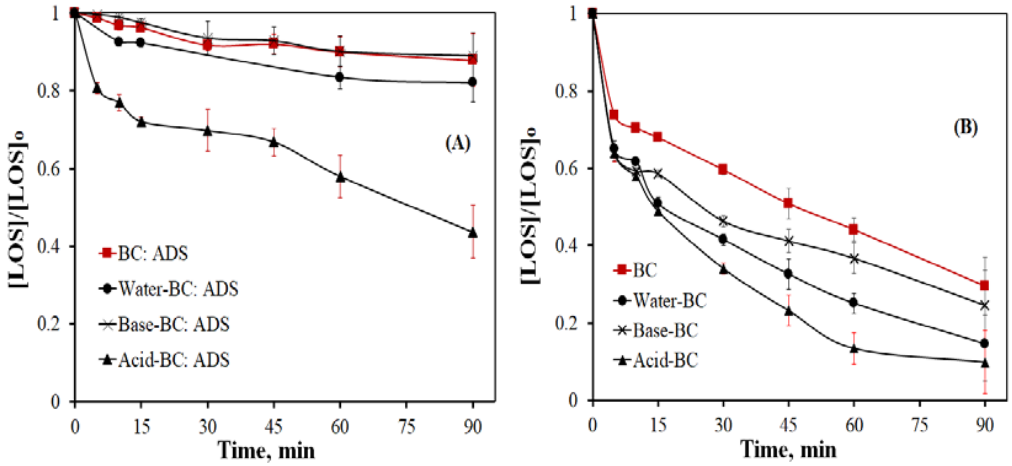

Figure 3. (**A**) LOS adsorption at inherent pH = 5.6 by untreated and treated biochar. (**B**) LOS degradation at inherent pH = 5.6 by biochar/SPS process. Experimental conditions (LOS) = 250 μg/L, (SPS) = 250 mg/L and (BC) = (water–BC) = (base–BC) = (acid–BC) = 90 mg/L in UPW.

The pKa of LOS is 5.05, indicating that it exists in a slightly deprotonated form at inherent pH ≈ 5.6 [23]. In addition, the results suggest that π–π interactions can play a significant role in the adsorption process, as has been supported in the literature [24–26]. Even in the case where π–π interactions are the primary mechanism, small pH changes may occur. This is due to the charge transfer from LOS to the biochar surface. In any case, it can be supported that the active sites are those that can exchange H^+ with LOS in order to equilibrate the system. It has been reported that releasing LOS from a surface demands an extremely low pH equal to 1.2 [27].

To test the oxidation ability of the four biochars, 250 mg/L SPS was added to the reactor. Figure 3B reveals that all biochars can activate SPS at inherent pH = 5.6, with the untreated one exhibiting the lower activity. This is preliminary evidence that the modification procedure can alter the activity of the biochar. It may partly be attributed to the enhancement of the modified BC's SSA. As seen in Figure 3B, the trend of LOS degradation efficiency matches that of adsorption, implying that adsorption is an essential factor since oxidation reactions are likely to occur on the biochar surface and/or on the interface. The 90 min LOS degradation is 70%, 76%, 84%, and 91% for BC, base–BC, water–BC, and acid–BC, respectively. Moreover, the LOS oxidation profile obeys pseudo-first-order kinetics (Equation (1)), with R^2 always greater than 0.95. The computed apparent rate constants (k_{app}, min^{-1}) are displayed in Table 2. Acid–BC k_{app} is 2.46, 2, and 1.52 times greater than the k_{app} of BC, base–BC, and water–BC, respectively.

$$\text{rate} = -\frac{d(LOS)}{dt} = k_{app}[LOS] \rightarrow [LOS] = (LOS)_o e^{-k_{app}t} \rightarrow \ln\left(\frac{[LOS]}{[LOS]_o}\right) = -k_{app}t \quad (1)$$

Since biochar treatment changes its surface acidity considerably (Table 1), it was decided that it was necessary to investigate the effect of initial pH on the adsorption and degradation of LOS; the results are shown in Figure 4. It is evident that the initial pH plays a significant role, affecting both the adsorption and degradation of LOS in all tested biochars. This supports the argument that the interplay amongst the surface, LOS, and the oxidant for the adsorption and degradation processes is not only through π–π interactions, but also electrostatic forces, since LOS removal declines as the solution pH increases from 3 to 10. Only in the case of acid–BC does LOS adsorption remain nearly constant at the acidic or near-neutral pH due to the release of H^+ from biochar and the acidification of the solution; this results in 56% of LOS removal after 90 min of adsorption at either condition (Figure 4D). However, at pH = 10, LOS adsorption is dramatically reduced to 6%.

Table 2. k_{app} values for 250 µg/L LOS adsorption and degradation for the studied biochars at initial pH 3, 5.6, and 10. Experimental conditions (biochar) = 90 mg/L and (SPS) = 250 mg/L in UPW.

Biochar	$pH_{initial}$	pH_{final} Oxid/Ads	$k_{oxidation}$, min^{-1}	$k_{adsorption}$, min^{-1}	$k_{oxidation}/k_{adsorption}$
BC	$pH_{inherent} \approx 5.6$	4.2/6.0	0.0142	0.0016	8.875
Water–BC	$pH_{inherent} \approx 5.6$	3.9/5.7	0.0230	0.0025	9.200
Base–BC	$pH_{inherent} \approx 5.6$	4.6/6.2	0.0170	0.0014	12.143
Acid–BC	$pH_{inherent} \approx 5.6$	3.8/4.5	0.035	0.0093	3.763
BC	3.0	3.0/3.0	0.0160	0.0099	1.616
Water–BC	3.0	3.0/3.0	0.0350	0.0166	2.108
Base–BC	3.0	3.0/3.0	0.0310	0.0196	1.582
Acid–BC	3.0	3.0/3.0	0.0090	0.0093	0.968
BC	10.0	9.4/9.9	0.0011	0.0009	1.222
Water–BC	10.0	9.8/97	0.0017	0.0006	2.833
Base–BC	10.0	10.0/9.7	0.0012	0.0003	4.000
Acid–BC	10.0	9.5/9.6	0.0026	0.0007	3.714

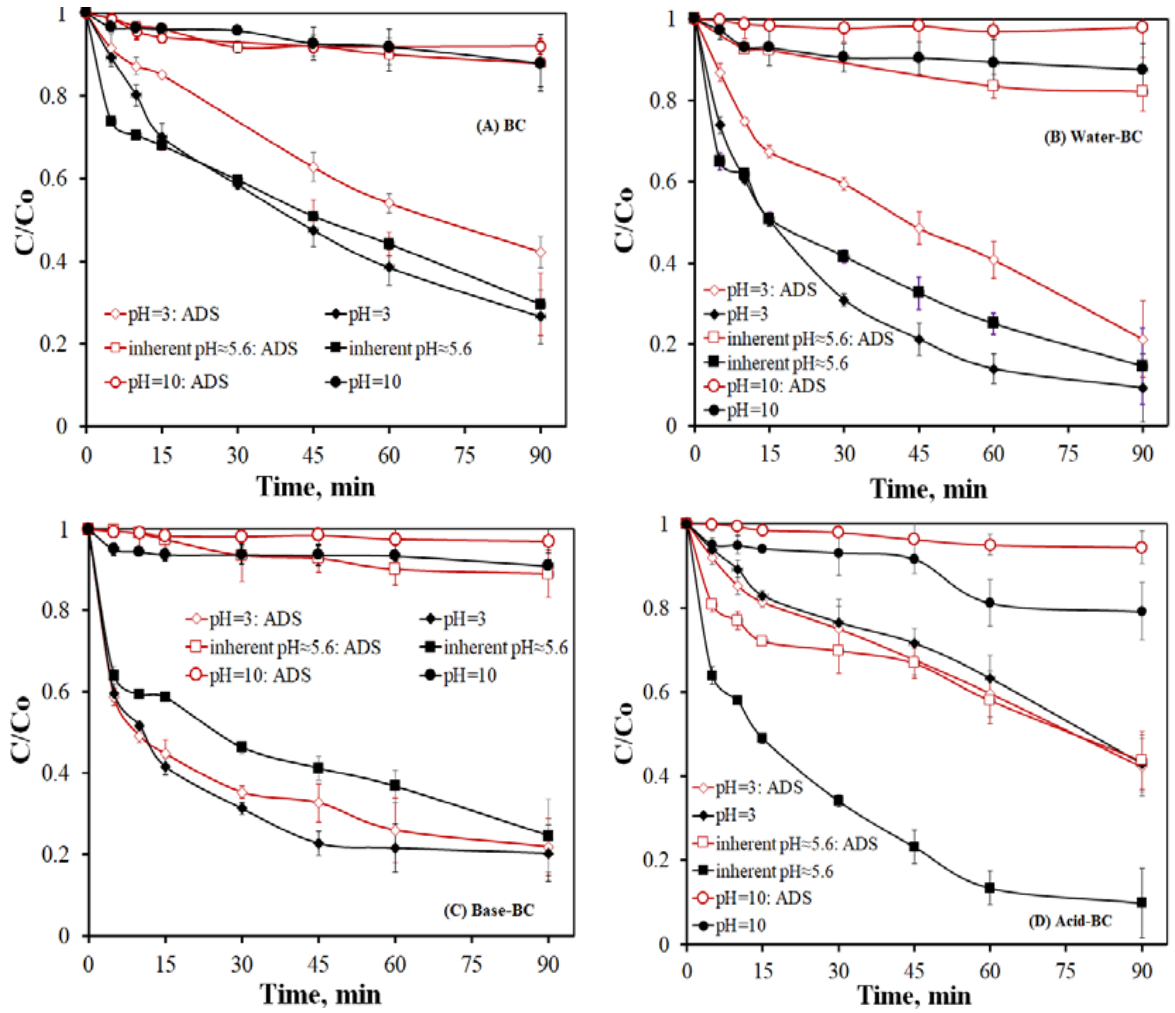

Figure 4. Effect of initial pH on 250 µg/L LOS degradation using 250 mg/L SPS and 90 mg/L of (**A**) BC, (**B**) water–BC, (**C**) base-BC, and (**D**) acid–BC in UPW. The corresponding adsorption experiments (without SPS) are also shown.

All other biochars exhibit a high degree of adsorption at acidic pH (water–BC: 79%, and base–BC: 80%). At this pH, the surface consumes a significant amount of H^+ and the surface is protonated, facilitating the release of H^+ during LOS adsorption. On the

other hand, and under basic conditions, the surface is negatively charged, and so is LOS. Thus, the observed decreased activity probably correlates with the repulsive electrostatic interactions, which seem to gain ground at alkaline conditions against the dominant π–π interactions at inherent pH and pH = 3 [25,28].

Figure 4 also shows that LOS oxidation upon the addition of 250 mg/L SPS is highly dependent on the solution pH. This is also demonstrated in Table 2, where the respective k_{app} values are reported. Although the protonated form of SPS is a weak acid with a pKa equal to 6.3 [29], the observed differences may be due to interactions between LOS and the biochar surface. Due to the high concentration of H^+ at pH = 3 and HO^- at pH = 10, only negligible changes in pH are recorded during the degradation process. Although, at inherent pH = 5.6, pH partially changes after 90 min of oxidation. Specifically, the final pH is 4.2, 3.9, 4.6, and 3.8 for BC, water–BC, base–BC, and acid–BC, respectively, i.e., lower than its starting value. This is due to the acidification of the solution during persulfate activation, which produces HSO_4^- as a side product—a medium-strong acid that lowers the solution pH.

Generally, LOS degradation decreases as the solution pH rises, as seen in Figure 4A–C and Table 2. For example, the 60 min remaining percentage of 250 μg/L LOS is 38%, 44%, and 91.7% for BC, 13.9%, 25%, and 89.3% for water–BC, and 21.6%, 36.7%, and 93.4% for base–BC at the initial pH equal to 3, 5.6, and 10, respectively. In the case of acid–BC (Figure 4D), LOS degradation is favored at inherent pH; it is noteworthy that the ratio of $k_{oxidation}$ to $k_{adsorption}$ (Table 2) at pH = 3 is nearly equal to 1, which implies that the biochar acts as an adsorbent rather than a persulfate activator. On the contrary, the ratio becomes 3.76 and 3.71 at pH = 5.6 and 10, respectively, demonstrating LOS oxidation. However, the process performance is very low at pH 10 due to the repulsive forces between acid–BC, LOS, and persulfate; only 20% of LOS removal is achieved after 90 min.

Similar results have been reported by Li et al., who studied the destruction of 20 mg/L of acid orange 7 at pH 10 with 10 g/L of rice-hull-derived biochar that had been modified with hydrofluoric acid [30]. Table 3 summarizes recent studies, where different research groups pyrolyzed various biomasses to synthesize biochar. The latter was modified with acid [30], base [31], plasma [32], or with a metal addition [33]. As seen in Table 3, the proposed eco-friendly-treated biochars are competitive compared to other modification strategies. Indeed, their efficiency is quite satisfactory, considering the experimental conditions used in this study (i.e., low biochar and persulfate concentration).

Table 3. Application of modified biochars for sulfate-radical activation for various pollutant decompositions.

Biomass Source	Modification Treatment	BC Concentration, mg/L	Oxidant, mg/L	Target Pollutant, mg/L	Removal, %	Ref.
Rice-hull	Hydrofluoric acid	10000	Persulfate, 1359	Acid orange 7, 20	70% in deionized water at 120 min	[30]
Pinewood	KOH	1000	Persulfate, 238	Carbamazepine, 5	40% in UPW at 60 min	[31]
Pine needle leaves	Plasma (250 W)	200	Peroxymonosulfate, 456.6	Phenol, 10	98% in deionized water at 120 min	[32]
Citrus peels	$Cu^0Fe_3O_4$@biochar (65%)	600	Peroxymonosulfate, 1000	Bisphenol A, 20	95% in deionized water at 120 min	[33]
Spent malt rootlet	H_2SO_4 NaOH Water	90	Persulfate, 250	Losartan, 0.25	91%, 76%, 84% in UPW at 90 min	This study

Of the various biochars tested, the acid–BC seems to be more efficient in terms of LOS removal by combined adsorption and oxidation processes. In this respect, its properties were further examined. Using EDX analysis, it was found that the acid–BC consists mainly of C (86.13% atomic ratio) and O (10.53%), while the rest are Si (0.12%), S (1.65%), Cl (0.23%),

and K (1.34%), with a uniform distribution. The high amount of S is due to the treatment with H_2SO_4, which creates $^{-}OSO_3H$ sites on the surface responsible for the acidic behavior of the biochar.

The XRD pattern of the acid–BC, presented in Figure S5A, shows a broad peak at 25.2° that can be assigned to the (002) crystal plane of hard carbon in lignocellulose form [34]. This peak is typical of carbonaceous material with a less ordered structure due to pyrolysis and is more intense than the peaks of the starting BC or those treated with base or water (Figure S6). However, it is less broad than the usual recorded peaks for biochars, and this may be attributed to the removal of cellulose and hemicellulose, which results in a more homogenous carbonaceous phase, where lignin is the main component. The second peak at 43.2° corresponds to the (100) crystal plane describing the graphitic structure from sp^2 orbitals, which improves electrical conductivity [35]. The FT–IR spectrum of the acid–BC sample, presented in Figure S5B, clearly shows the presence of oxo groups. The broad peak centered at 3454 cm^{-1} is due to the surface –OH groups and adsorbed H_2O molecules, while the peak at 1114 cm^{-1} is due to the C–O bonds. The peak at 1627 cm^{-1} can be attributed to the C=C bond in the aromatic structure. The aromatic phase is poor in H since no peaks corresponding to C–H in the aromatic form (wavenumbers higher than 3000 cm^{-1}) were detected. The slight shift in the C=C bond denotes that π electrons are in conjugation [36] by functional groups with high electronegativity. Finally, the peak at 1391 cm^{-1} is due to $–SO_3H$ groups, although the intensity of the band is rather low [37]. Generally, the low intensity of the peaks in the region of 1000–1800 cm^{-1} is characteristic of the heterogeneity of the biochar. [13,38,39]. The differences with the other three biochars (Figure S7) are not so intense, as in the case of the XRD and TGA results.

The acid–base behavior of acid–BC was studied with potentiometric titrations, and it was found that the pzc is less than 2.5. After the first titration, acid–BC was collected by filtration, washed with ultrapure water, and the titration was repeated for a second cycle to check the stability of the $–OSO_3H$ groups. The results are presented in Figure 5, confirming the surface group's stability and their participation in reversible acid–base reactions. The H^+ consumption curve, presented in Figure 6a, reveals that the biochar is negatively charged in the whole pH range studied. This charge progressively increases with the pH. The lower value of the H^+ consumed, and thus, the surface charge, occurs at a pH value of approximately 3.8. The differential curve (Figure 6b) of the H^+ consumed confirms this observation, indicating that the acidic surface groups have a pK value close to 3. These sites are not present in the starting biochar and result from the acid treatment [17].

This explains why the majority of the surface sites are protonated at pH = 3 and, thus, explains the higher activity for LOS uptake. As has been discussed earlier, the sites involved in LOS removal are those that can be protonated at the beginning and then deprotonated after the interaction with LOS. Interestingly, the speciation of the surface sites for the acid–BC shows that they are homogeneous with a pK equal to 3.

The participation of these surface sites and the release of H^+ in the solution during LOS removal is confirmed with the correlation of the k_{app} values with the difference in pH values (ΔpH: pH_{fin_ox}-pH_{fin_ads}) between the adsorption and oxidation processes. Changes in solution pH are due to the (i) addition of biochar, (ii) adsorption of LOS, and (iii) activation of SPS. The addition of BC shifts pH to the pzc of the biochar since the acidic or basic groups are added in the solution. The adsorption of LOS shifts the pH to lower values since the accumulation of LOS on the surface releases H^+ in the solution. Finally, SPS activation lowers the pH significantly, as HSO_4^- is produced. The last process is closely related to oxidation; the lower the pH, the higher the amount of SPS activated.

Therefore, the net influence of pH on oxidation should be derived from the subtraction of the two pH values between the adsorption and oxidation processes. Indeed, the linear correlation between the k_{app} and ΔpH, as presented in Figure 7, confirms the assumption.

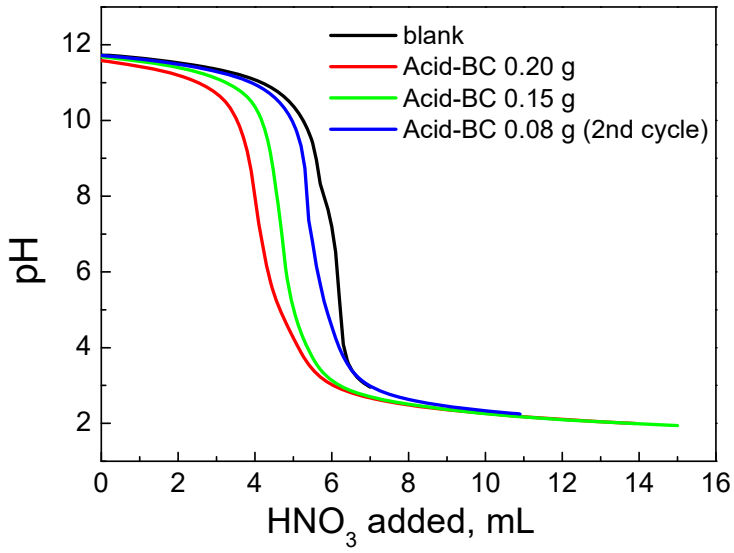

Figure 5. Titrations curves for the blank solution and two suspensions of biochar with 0.15 and 0.2 g. The third titration curve (blue line) corresponds to the second titration of a previously titrated sample after filtration and washing with ultrapure water.

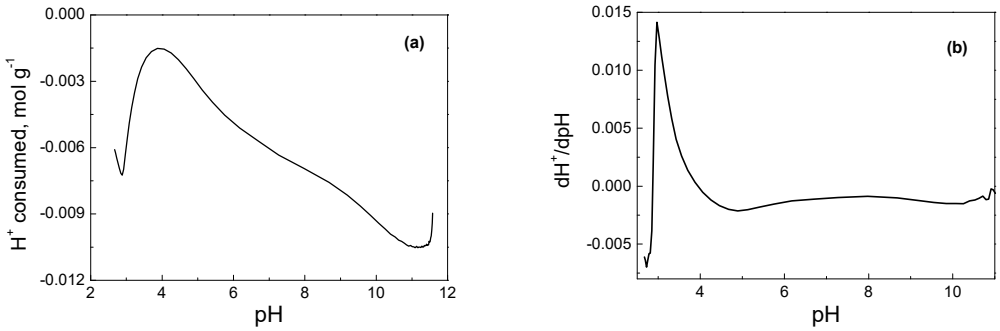

Figure 6. (**a**) H^+ consumed by the surface as a function of the solution pH; (**b**) the differential curve of the H^+ consumed with pH.

To explore the contribution of reactive species such as sulfate radical ($SO_4^{\cdot-}$), hydroxyl radical ($HO^{\cdot}$), and singlet oxygen ($^1O_2$) in the oxidation process of 250 µg/L LOS, 100 mM methanol, 100 mM t-butanol, and 1.54 mM sodium azide were used as scavengers for $SO_4^{\cdot-}$, $HO^{\cdot}$, and $^1O_2$, respectively. Methanol is considered an effective scavenger for both $SO_4^{\cdot-}$ and $HO^{\cdot}$, although its reaction rate constant with $SO_4^{\cdot-}$ is approximately 100 times greater than the respective value with $HO^{\cdot}$ [40,41]. On the other hand, t-butanol reacts almost 1000 times faster with $HO^{\cdot}$ than $SO_4^{\cdot-}$ [42], thus, it is regarded mainly as a $HO^{\cdot}$ scavenger [42]. NaN_3 has been reported as a sufficient scavenger of $^1O_2$ with a kinetic constant in the order of 10^9 [24,42,43]. As seen in Figure 8, the addition of 100 mM of either t-butanol or methanol partially impedes LOS degradation in a similar manner, confirming the formation and participation of both free radicals in LOS decomposition. Specifically, the 90 min LOS removal declines from 90% without scavenger to 64% in the presence of either alcohol, while the k_{app} value is reduced 2.6-fold. The fact that an excess of alcohol cannot completely hinder degradation implies that species other than sulfate and hydroxyl radicals may be involved in the reaction; this seems to be the case, since the addition of sodium azide leads to a 5.4-fold decrease in the degradation rate, verifying that a non-radical pathway driven by singlet oxygen significantly participates in LOS elimination.

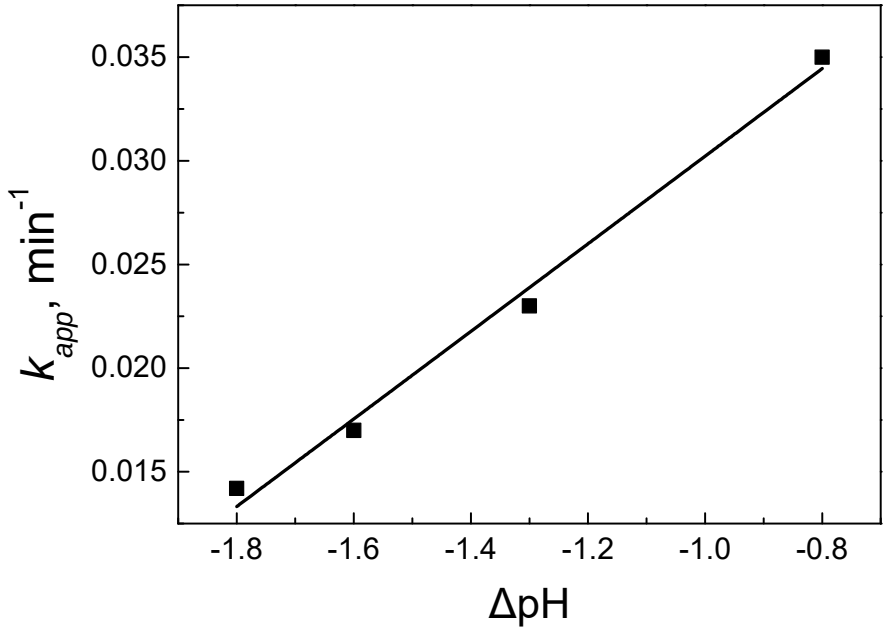

Figure 7. Linear correlation between k_{app} of the biochars at inherent pH with the pH difference between adsorption and oxidation processes.

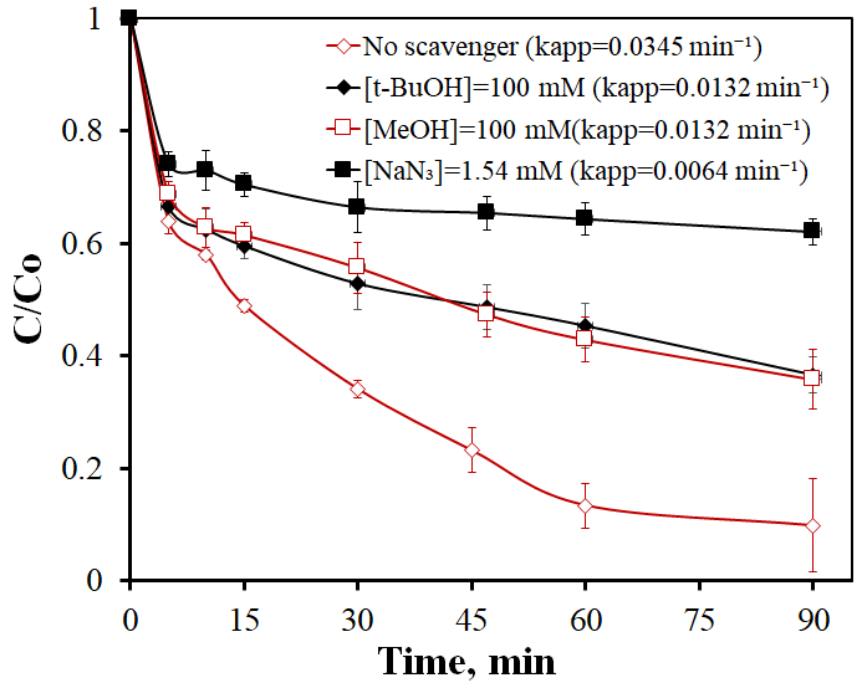

Figure 8. LOS degradation without and with radical scavengers. Experimental conditions: (LOS) = 250 μg/L, (SPS) = 250 mg/L, (acid–BC) = 90 mg/L in UPW.

Similar findings regarding the role of non-radical pathways in the degradation of micropollutants have been reported by Avramiotis et al. [18], who studied the degradation of sulfamethoxazole by rice husk biochar and persulfate, and de Andrade et al. [43], who examined the degradation of losartan by N-doped hierarchical porous carbon and peroxymonosulfates.

A final experiment was performed to assess process performance in a real water matrix, i.e., the secondary-treated wastewater (WW) taken from the University of Patras campus treatment plant; the results are shown in Figure 9. The detrimental effect of the

non-target species naturally present in WW (effluent organic matter, inorganic ions) is evident irrespective of the initial matrix pH; such species compete with LOS for the active sites of biochar, as well as the various reactive oxygen species. This rather complicated interplay decreases performance through secondary, unwanted reactions.

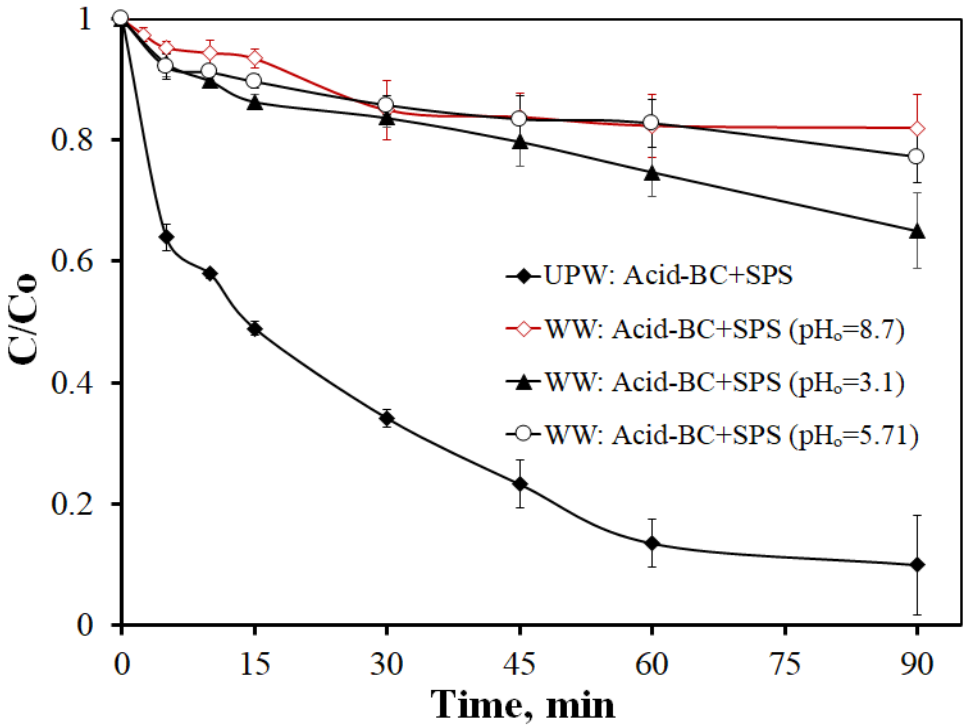

Figure 9. Effect of wastewater (WW) on LOS degradation at several pH values. Experimental conditions: (LOS) = 250 μg/L, (SPS) = 250 mg/L, (acid–BC) = 90 mg/L.

3. Materials and Methods

3.1. Reagents Used

All materials used in this study were purchased from Sigma Aldrich (St. Louis, MO, USA), unless otherwise noted.

3.2. Biochar Preparation

The raw biochar was prepared by pyrolysis of spent malt rootlets, and was provided by the Athenian Brewery S.A. (Patras, Greece). After overnight drying at 50 °C and sieving into 1.18–0.15 mm, biomass was placed into custom-made quartz vessels and heated to 850 °C in a gradient temperature furnace (LH 60/12, Nabertherm GmbH, Lilienthal, Germany). The pyrolysis was performed under a limited O_2 atmosphere, i.e., approximately 20% of the O_2 required for the total burning of the raw biomass. Experimental details for the modification of the catalysts can be found in a previous study [22]. Briefly, an amount of BC from spent malt rootlets was prepared at 850 °C under a limited oxygen atmosphere. For the modification procedure, a proper amount of this BC was heated with the acid (H_2SO_4 1M), base (NaOH 1M), or water solution under reflux for 30 min. The ratio of the solid to liquid was 0.017. After heating, the suspension was cooled, filtered, washed with 1 L of 3D H_2O, and dried at 120 °C for 120 min.

3.3. Physicochemical Characterization

The starting and modified samples were characterized with various physicochemical techniques. The adsorption isotherm of N_2 at the liquid N_2 temperature (–196 °C) was used to determine the specific surface area (SSA), micropore surface area, and the pore-size distribution. A scanning electron microscope (SEM) (FEI Quanta 250 FEG, Thermo Fisher

Scientific Inc., Waltham, MA, USA) working under different pressures (10–4000 Pa) was used for the SEM images of the sample, while FTIR spectra were recorded as % wt/wt biochar in KBr pellets in the region of 4000–400 cm^{-1} (Perkin Elmer Spectrum RX FTIR spectrometer, Waltham, MA, USA). A Bruker D8 Advance diffractometer (Billerica, MA, USA), equipped with nickel-filtered CuKa (1.5418 Å) radiation was used for collecting the X–ray diffraction (XRD) patterns. Thermogravimetric analysis (TGA) was performed in a TGA Perkin Elmer system under an air atmosphere with 20 mL/min flow. Finally, the point of zero-charge determination was performed using the potentiometric mass titration (PMT) method [44], (TIM 800 Radiometer Copenhagen Autoburette System equipped with the Timtalk 8, version 2.0 software). More details about the experimental part can be found in the literature [45,46].

3.4. Oxidation Experiments and Losartan Measurement

Experiments were conducted in a glass reactor with 120 mL working volume at room temperature to evaluate catalytic activity [11,13]. The initial concentration of the drug losartan was fixed at 250 μg/L, and ultrapure water (UPW) from a Millipore unit was used as the water matrix (unless otherwise stated). The biochar concentration was 90 mg/L, and the persulfate concentration was 250 mg/L. The initial pH was adjusted for some experiments using 1 M NaOH or 1 M H_2SO_4 without buffer addition to avoid possible interferences. Additional experiments were conducted using the secondary effluent derived from the wastewater treatment plant of the University of Patras Campus, and the physicochemical characterization can be found elsewhere [23].

Samples were withdrawn from the reactor (1.2 mL), quenched with 0.3 mL methanol, filtered using a PVDF 0.22 μm syringe filter, and introduced to Waters Alliance 2695 HPLC. LOS was measured using Water 2996 Photodiode Array Detector and operated at 220 nm. More details regarding the analytical measurements can be found in a previous study [23].

4. Conclusions

The main findings derived from this work are summarized as follows:

- A mild treatment of biochars (i.e., low temperature and dilute acid or base) is capable of significantly altering its physicochemical properties. The effect is more pronounced on the surface area, the pzc, and the concentration of minerals.
- From the various samples tested, the acid-treated BC generally exhibits the highest efficiency. Conversely, oxidation is significantly delayed at alkaline conditions and/or in a complex secondary effluent. This material behaves predominantly as an adsorbent in acidic conditions and becomes a persulfate activator at near-neutral and alkaline environments.
- Indirect scavenging experiments confirm the contribution of a non-radical mechanism (singlet oxygen) in addition to the radical pathways induced by sulfate and hydroxyl radicals.

In a nutshell, this work has clearly demonstrated that there is no need for extreme conditions to modify catalytic materials, such as biochars, in order to enhance their activity and tune the mechanisms of action. This work has made an attempt to correlate properties to activity, which is important for valorizing waste materials in a rational fashion. Waste valorization promotes the concept of circular economy, and this requires properly designed materials with a reduced environmental and energy footprint. In this view, more research should be carried out in directions such as the stability and reusability of such materials for large-scale applications.

Supplementary Materials: The following supporting information can be downloaded at: https://www.mdpi.com/article/10.3390/catal12101245/s1, Figures S1–S4: SEM images of the samples, Figure S5: XRD pattern (A) and FTIR spectrum (B) of the acid-treated BC, Figure S6: XRD patterns of the pristine BC and the base- and water-treated samples and Figure S7: FTIR spectra of the pristine BC and the base- and water-treated samples.

Author Contributions: Conceptualization, J.V., D.M. and Z.F.; methodology, J.V. and Z.F.; formal analysis, J.V. and A.A.I.; investigation, A.A.I. and J.V.; resources, D.M.; data curation, A.A.I. and J.V.; writing—original draft preparation, A.A.I., J.V., Z.F. and D.M.; writing—review and editing, D.M.; visualization, A.A.I. and J.V.; supervision, D.M.; funding acquisition, D.M. All authors have read and agreed to the published version of the manuscript.

Funding: A.A.I. acknowledges that this work is part of the project "Hybrid oxidation processes in tertiary wastewater treatment", which is implemented under the Action "H.F.R.I.—2nd Call of Scholarships H.F.R.I for PhD Candidates" funded by H.F.R.I. Hellenic Foundation for Research and Innovation (Fellowship Number: 1281).

Data Availability Statement: The data presented in this study are available on request from the corresponding author.

Acknowledgments: I.D. Manariotis is gratefully acknowledged for providing the starting biochar.

Conflicts of Interest: The authors declare no conflict of interest.

References

1. Sauvé, S.; Bernard, S.; Sloan, P. Environmental sciences, sustainable development and circular economy: Alternative concepts for trans-disciplinary research. *Environ. Dev.* **2016**, *17*, 48–56. [CrossRef]
2. Romanovski, V. Chapter 25- Agricultural waste based-nanomaterials: Green technology for water purification. In *Micro and Nano Technologies*; Abd-Elsalam, K.A., Zahid, M., Eds.; Aquananotechnology; Elsevier: Amsterdam, The Netherlands, 2021; pp. 577–595. ISBN 9780128211410. [CrossRef]
3. Ganesh, K.S.; Sridhar, A.; Vishali, S. Utilization of fruit and vegetable waste to produce value-added products: Conventional utilization and emerging opportunities—A review. *Chemosphere* **2022**, *287*, 132221. [CrossRef]
4. Wang, J.; Wang, S. Preparation, modification and environmental application of biochar: A review. *J. Clean. Prod.* **2019**, *227*, 1002–1022. [CrossRef]
5. Zhang, A.; Li, X.; Xing, J.; Xu, G. Adsorption of potentially toxic elements in water by modified biochar: A review. *J. Environ. Chem. Eng.* **2020**, *8*, 104196. [CrossRef]
6. Cheng, N.; Wang, B.; Wu, P.; Lee, X.; Xing, Y.; Chen, M.; Gao, B. Adsorption of emerging contaminants from water and wastewater by modified biochar: A review. *Environ. Pollut.* **2021**, *273*, 116448. [CrossRef] [PubMed]
7. Liu, D.; Gu, W.; Zhou, L.; Wang, L.; Zhang, J.; Liu, Y.; Lei, J. Recent advances in MOF-derived carbon-based nanomaterials for environmental applications in adsorption and catalytic degradation. *Chem. Eng. J.* **2022**, *427*, 131503. [CrossRef]
8. Guo, D.; You, S.; Li, F.; Liu, Y. Engineering carbon nanocatalysts towards efficient degradation of emerging organic contaminants via persulfate activation: A review. *Chinese Chem. Lett.* **2022**, *33*, 1–10. [CrossRef]
9. Dimitriadou, S.; Frontistis, Z.; Petala, A.; Bampos, G.; Mantzavinos, D. Carbocatalytic activation of persulfate for the removal of drug diclofenac from aqueous matrices. *Catal. Today* **2020**, *355*, 937–944. [CrossRef]
10. Bekris, L.; Frontistis, Z.; Trakakis, G.; Sygellou, L.; Galiotis, C.; Mantzavinos, D. Graphene: A new activator of sodium persulfate for the advanced oxidation of parabens in water. *Water Res.* **2017**, *126*, 111–121. [CrossRef] [PubMed]
11. Kemmou, L.; Frontistis, Z.; Vakros, J.; Manariotis, I.D.; Mantzavinos, D. Degradation of antibiotic sulfamethoxazole by biochar-activated persulfate: Factors affecting the activation and degradation processes. *Catal. Today* **2018**, *313*, 128–133. [CrossRef]
12. Zhao, Y.; Yuan, X.; Li, X.; Jiang, L.; Wang, H. Burgeoning prospects of biochar and its composite in persulfate-advanced oxidation process. *J. Hazard. Mater.* **2021**, *409*, 124893. [CrossRef]
13. Magioglou, E.; Frontistis, Z.; Vakros, J.; Manariotis, I.D.; Mantzavinos, D. Activation of Persulfate by Biochars from Valorized Olive Stones for the Degradation of Sulfamethoxazole. *Catalysts* **2019**, *9*, 419. [CrossRef]
14. Huang, B.C.; Jiang, J.; Huang, G.X.; Yu, H.Q. Sludge biochar-based catalysts for improved pollutant degradation by activating peroxymonosulfate. *J. Mater. Chem. A* **2018**, *6*, 8978–8985. [CrossRef]
15. Lykoudi, A.; Frontistis, Z.; Vakros, J.; Manariotis, I.D.; Mantzavinos, D. Degradation of sulfamethoxazole with persulfate using spent coffee grounds biochar as activator. *J. Environ. Manage.* **2020**, *271*, 111022. [CrossRef]
16. Song, G.; Qin, F.; Yu, J.; Tang, L.; Pang, Y.; Zhang, C.; Wang, J.; Deng, L. Tailoring biochar for persulfate-based environmental catalysis: Impact of biomass feedstocks. *J. Hazard. Mater.* **2022**, *424*, 127663. [CrossRef] [PubMed]
17. Grilla, E.; Vakros, J.; Konstantinou, I.; Manariotis, I.D.; Mantzavinos, D. Activation of persulfate by biochar from spent malt rootlets for the degradation of trimethoprim in the presence of inorganic ions. *J. Chem. Technol. Biotechnol.* **2020**, *95*, 2348–2358.
18. Avramiotis, E.; Frontistis, Z.; Manariotis, I.D.; Vakros, J.; Mantzavinos, D. On the Performance of a Sustainable Rice Husk Biochar for the Activation of Persulfate and the Degradation of Antibiotics. *Catalysts* **2021**, *11*, 1303. [CrossRef]
19. Azargohar, R.; Dalai, A.K. Steam and KOH activation of biochar: Experimental and modeling studies. *Microporous Mesoporous Mater.* **2008**, *110*, 413–421. [CrossRef]
20. Xia, D.; Tan, F.; Zhang, C.; Jiang, X.; Chen, Z.; Li, H.; Zheng, Y.; Li, Q.; Wang, Y. $ZnCl_2$-activated biochar from biogas residue facilitates aqueous As(III) removal. *Appl. Surf. Sci.* **2016**, *377*, 361–369. [CrossRef]

21. Zhu, L.; Zhao, N.; Tong, L.; Lv, Y. Structural and adsorption characteristics of potassium carbonate activated biochar. *RSC Adv.* **2018**, *8*, 21012–21019. [CrossRef]
22. Ntaflou, M.; Vakros, J. Transesterification activity of modified biochars from spent malt rootlets using triacetin. *J. Clean. Prod.* **2020**, *259*, 120931. [CrossRef]
23. Ioannidi, A.; Arvaniti, O.S.; Nika, M.-C.; Aalizadeh, R.; Thomaidis, N.S.; Mantzavinos, D.; Frontistis, Z. Removal of drug losartan in environmental aquatic matrices by heat-activated persulfate: Kinetics, transformation products and synergistic effects. *Chemosphere* **2022**, *287*, 131952. [CrossRef] [PubMed]
24. Avramiotis, E.; Frontistis, Z.; Manariotis, I.D.; Vakros, J.; Mantzavinos, D. Oxidation of Sulfamethoxazole by Rice Husk Biochar-Activated Persulfate. *Catalysts* **2021**, *11*, 850. [CrossRef]
25. Tang, H.; Zhao, Y.; Shan, S.; Yang, X.; Liu, D.; Cui, F.; Xing, B. Theoretical insight into the adsorption of aromatic compounds on graphene oxide. *Environ. Sci. Nano* **2018**, *5*, 2357–2367. [CrossRef]
26. Mrozik, W.; Minofar, B.; Thongsamer, T.; Wiriyaphong, N.; Khawkomol, S.; Plaimart, J.; Vakros, J.; Karapanagioti, H.; Vinitnantharat, S.; Werner, D. Valorisation of agricultural waste derived biochars in aquaculture to remove organic micropollutants from water—experimental study and molecular dynamics simulations. *J. Environ. Manag.* **2021**, *300*, 113717. [CrossRef]
27. Ejsmont, A.; Stasiłowicz-Krzemień, A.; Ludowicz, D.; Cielecka-Piontek, J.; Goscianska, J. Synthesis and Characterization of Nanoporous Carbon Carriers for Losartan Potassium Delivery. *Materials* **2021**, *14*, 7345. [CrossRef]
28. Ren, W.; Xiong, L.; Yuan, X.; Yu, Z.; Zhang, H.; Duan, X.; Wang, S. Activation of Peroxydisulfate on Carbon Nanotubes: Electron-Transfer Mechanism. *Environ. Sci. Technol.* **2019**, *53*, 14595–14603. [CrossRef]
29. Ioannidi, A.; Frontistis, Z.; Mantzavinos, D. Destruction of propyl paraben by persulfate activated with UV-A light emitting diodes. *J. Environ. Chem. Eng.* **2018**, *6*, 2992–2997. [CrossRef]
30. Li, F.; Xie, Y.; Wang, Y.; Fan, X.; Cai, Y.; Mei, Y. Improvement of dyes degradation using hydrofluoric acid modified biochar as persulfate activator. *Environ. Pollut. Bioavailab.* **2019**, *31*, 32–37. [CrossRef]
31. Xue, Y.; Guo, Y.; Zhang, X.; Kamali, M.; Aminabhavi, T.M.; Appels, L.; Dewil, R. Efficient adsorptive removal of ciprofloxacin and carbamazepine using modified pinewood biochar—A kinetic, mechanistic study. *Chem. Eng. J.* **2022**, *450*, 137896. [CrossRef]
32. Liu, X.; Zhou, J.; Liu, D. Plasma regulates active sites on biochar to boost peroxomonosulfate activation for phenol degradation. *J. Environ. Chem. Eng.* **2022**, *10*, 107833. [CrossRef]
33. Chen, K.; Zhou, L.; Xu, W.; Hu, Z.; Jia, M.; Liu, L. A novel way of activating peroxysulfate by zero-valent copper and ferroferric oxide co-modified biochar to remove bisphenol A in aqueous solution: Performance, mechanism and potential toxicity. *Appl. Catal. A Gen.* **2022**, *636*, 118575. [CrossRef]
34. Qian, L.; Guo, F.; Jia, X.; Zhan, Y.; Zhou, H.; Jiang, X.; Tao, C. Recent development in the synthesis of agricultural and forestry biomass-derived porous carbons for supercapacitor applications: A review. *Ionics* **2020**, *26*, 3705–3723. [CrossRef]
35. Gao, G.; Cheong, L.Z.; Wang, D.; Shen, C. Pyrolytic carbon derived from spent coffee grounds as anode for sodium-ion batteries. *Carbon Resour. Convers.* **2018**, *1*, 104–108. [CrossRef]
36. Kaczmarczyk, B. FTIR study of conjugation in selected aromatic polyazomethines. *J. Mol. Struct.* **2013**, *1048*, 179–184. [CrossRef]
37. Suganuma, S.; Nakajima, K.; Kitano, M.; Yamaguchi, D.; Kato, H.; Hayashi, S.; Hara, M. Hydrolysis of Cellulose by Amorphous Carbon Bearing SO_3H, COOH, and OH Groups. *J. Am. Chem. Soc.* **2008**, *130*, 12787–12793. [CrossRef]
38. Tala, W.; Chantara, S. Use of spent coffee ground biochar as ambient PAHs sorbent and novel extraction method for GC–MS analysis Environ. *Sci. Poll. Res.* **2019**, *26*, 13025–13040. [CrossRef]
39. Ballesteros, L.F.; Teixeira, J.A.; Mussatto, S.I. Chemical, functional, and structural properties of spent coffee grounds and coffee silverskin. *Food Bioprocess Technol.* **2014**, *7*, 3493–3503. [CrossRef]
40. McElroy, W.J. A laser photolysis study of the reaction of sulfate (1-) with chloride and the subsequent decay of chlorine (1-) in aqueous solution. *J. Phys. Chem.* **1990**, *94*, 2435–2441. [CrossRef]
41. Jayson, G.G.; Parsons, B.J.; Swallow, A.J. Some simple, highly reactive, inorganic chlorine derivatives in aqueous solution. Their formation using pulses of radiation and their role in the mechanism of the Fricke dosimeter. *J. Chem. Soc. Faraday Trans. 1* **1973**, *69*, 1597. [CrossRef]
42. Ghanbari, F.; Moradi, M. Application of peroxymonosulfate and its activation methods for degradation of environmental organic pollutants: Review. *Chem. Eng. J.* **2017**, *310*, 41–62. [CrossRef]
43. de Andrade, J.R.; Vieira, M.G.A.; da Silva, M.G.C.; Wang, S. Oxidative degradation of pharmaceutical losartan potassium with N-doped hierarchical porous carbon and peroxymonosulfate. *Chem. Eng. J.* **2020**, *382*, 122971. [CrossRef]
44. Bourikas, K.; Vakros, J.; Kordulis, C.; Lycourghiotis, A. Potentiometric Mass Titrations: Experimental and Theoretical Establishment of a New Technique for Determining the Point of Zero Charge (PZC) of Metal (Hydr)Oxides. *J. Phys. Chem. B* **2003**, *107*, 9441–9451. [CrossRef]
45. Papatheodorou, G.; Ntzoufra, P.; Hapeshi, E.; Vakros, J.; Mantzavinos, D. Hybrid Biochar/Ceria Nanomaterials: Synthesis, Characterization and Activity Assessment for the Persulfate-Induced Degradation of Antibiotic Sulfamethoxazole. *Nanomaterials* **2022**, *12*, 194. [CrossRef] [PubMed]
46. Ntzoufra, P.; Vakros, J.; Frontistis, Z.; Tsatsos, S.; Kyriakou, G.; Kennou, S.; Manariotis, I.D.; Mantzavinos, D. Effect of Sodium Persulfate Treatment on the Physicochemical Properties and Catalytic Activity of Biochar Prepared from Spent Malt Rootlets. *J. Environ. Chem. Eng.* **2021**, *9*, 105071. [CrossRef]